



Stellenbosch
UNIVERSITY
IYUNIVESITHI
UNIVERSITEIT

forward together
sonke siya phambili
saam vorentoe

Design (E) 344 Report

Sameer Shaboodien
25002783

Report submitted in partial fulfilment of the requirements of the module
Design (E) 344 for the degree Baccalaureus in Engineering in the Department of Electrical
and Electronic Engineering at Stellenbosch University.

October 8, 2023



UNIVERSITEIT • STELLENBOSCH • UNIVERSITY
jou kennisvennoot • your knowledge partner

Plagiaatverklaring / *Plagiarism Declaration*

1. Plagiaat is die oorneem en gebruik van die idees, materiaal en ander intellektuele eiendom van ander persone asof dit jou eie werk is.

Plagiarism is the use of ideas, material and other intellectual property of another's work and to present is as my own.

2. Ek erken dat die pleeg van plagiaat 'n strafbare oortreding is aangesien dit 'n vorm van diefstal is.

I agree that plagiarism is a punishable offence because it constitutes theft.

3. Ek verstaan ook dat direkte vertalings plagiaat is.


I also understand that direct translations are plagiarism.

4. Dienooreenkomstig is alle aanhalings en bydraes vanuit enige bron (ingesluit die internet) volledig verwys (erken). Ek erken dat die woordelike aanhaal van teks sonder aanhalingstekens (selfs al word die bron volledig erken) plagiaat is.

Accordingly all quotations and contributions from any source whatsoever (including the internet) have been cited fully. I understand that the reproduction of text without quotation marks (even when the source is cited) is plagiarism

5. Ek verklaar dat die werk in hierdie skryfstuk vervat, behalwe waar anders aangedui, my eie oorspronklike werk is en dat ek dit nie vantevore in die geheel of gedeeltelik ingehandig het vir bepunting in hierdie module/werkstuk of 'n ander module/werkstuk nie.

I declare that the work contained in this assignment, except where otherwise stated, is my original work and that I have not previously (in its entirety or in part) submitted it for grading in this module/assignment or another module/assignment.

25002783	
Studentenommer / <i>Student number</i>	Handtekening / <i>Signature</i>
S. Shaboodien	October 8, 2023
Voorletters en van / <i>Initials and surname</i>	Datum / <i>Date</i>

Contents

Declaration	i
List of Figures	iv
List of Tables	v
Nomenclature	vi
1. 3.3V Voltage regulation	1
1.1. Introduction and Literature	1
1.2. Design	2
1.3. Simulated results	3
1.4. Measured results	3
1.5. Summary	3
2. Temperature sensor	4
2.1. Literature	4
2.2. Design	5
2.3. Simulated Results	6
2.4. Measured Results	7
2.5. Conclusion	7
3. Temperature sensor	8
3.1. Literature	8
3.2. Design	10
3.3. Simulation	10
3.4. Measured Results	11
3.5. Conclusion	11
4. Pedometer	12
4.1. Literature	12
4.2. Design	13
4.3. Measurements	15
4.4. Conclusion	15
5. Heartbeat Sensor	16
5.1. Literature	16
5.2. Design	17

5.2.1. Heart rate sensor circuit	17
5.2.2. Filter stage	17
5.2.3. Gain stage	18
5.2.4. Comparator stage	18
5.3. Simulated Results	19
5.4. Measured Results	19
5.5. Conclusion	20
6. System Overview	21
Bibliography	22
A. Social contract	23
B. GitHub Activity Heatmap	24
C. Reference figures	25

List of Figures

1.1. LM317 regulator standard application circuit	1
1.2. LM317 full 3.3V regulator circuit	2
2.1. Thin Film RTD	4
2.2. Analog temperature sensor configuration circuit	5
2.3. Analog temperature sensor simulated output	6
2.4. Sub-figures showing stable DC voltages and noise characteristics	7
3.1. Combined figure	9
3.2. Simulated results for different weights over time	11
4.1. Flow diagram of the code	14
4.2. Step measurements for each axis and noise measurement	15
5.1. Working of PPG heart rate sensor	17
5.2. Heart Rate Sensor Circuit	17
5.3. Heart Rate signal Conditioning Circuit	18
5.4. Heart Rate input signal of author	19
5.5. Simulation output vs conditioned input	19
5.6. Simulation circuitry current usage	19
5.7. Measured pulse output vs heart rate input	20
5.8. Input (CH1) vs output (CH2) noise	20
6.1. System Overview	21

List of Tables

2.1. Resistance and required output Voltage at Different Temperatures as per project specifications	6
2.2. Resistance and Output Voltage at Different Temperatures in simulation	7
4.1. MPPA Values for Walking and Running	13
4.2. Expected voltage values for different positive accelerations in each direction . .	13

Nomenclature

Variables and functions

V	Voltage.
I	Current.
C	Capacitance.
$R(T)$	Resistance as a function of temperature

Acronyms and abbreviations

V	volt
FVDC	fixed voltage division circuit
RTD	Resistance Temperature Detector
A	Ampere
PPG	photoplethysmography
BPM	Beats per Minute
F	Farad
μ	micro
m	milli
Ω	Ohm
EMI	Electromagnetic Inteference
op amp	operational amplifier
ΔR	weight driven individual load cell resistance change.
w	weight per cell
ΔV	weight driven voltage change per cell.
R_pushorpull	resistance for a push or pull resistor cell.
lhs	left-hand-side.
rhs	right-hand-side.
V_noweighthalf	lhs no weight centre node voltage.
V_totalchange	change in voltage per weight at lhs centre node.

Chapter 1

3.3V Voltage regulation

1.1. Introduction and Literature

This chapter will introduce the design steps and implementation of the 3.3V voltage regulator. The regulators purpose will involve converting down a 12V input into a 3.3V signal within 0.5% error at steady-state. This section will compare linear and switch mode voltage regulators, using the the LM317 [1] and the LM2576 [2] respectively.

How they work

Linear regulators work by having a circuit with variable resistance elements allowing control of the output voltage. Consequentially, power losses are proportional to the internal voltage drop (input voltage - output voltage) resulting in an inefficient regulator [3].

On the other hand, switching regulators turn on (minimal path resistance) and off (very low current flow) at a certain rate to control the output voltage. This means that the power dissipation is independent of the voltage drop resulting in a highly efficient regulator [3].

Both regulators are not designed to supply current for high power devices (e.g. 5A) and external current amplifiers are used if needed. Both regulators provide a regulated (stable) current whose value depends on the load as per their datasheets [1], [2].

Linear regulators tend to be cheaper [4] and have lower noise due to the lack of switching and as such are chosen for this application.

The standard application circuit for the LM317 as derived from [1] was utilized and is shown as follows in figure 1.1:

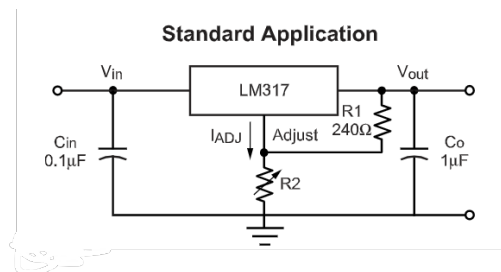


Figure 1.1: LM317 regulator standard application circuit

AND pics onto next page overload chapter 2 xxx AND // vs
AND search in appendix AND check literature pics

1.2. Design

The complete circuit is shown below in figure 1.2 which has been derived from the standard application circuit with changes explained following the diagram.

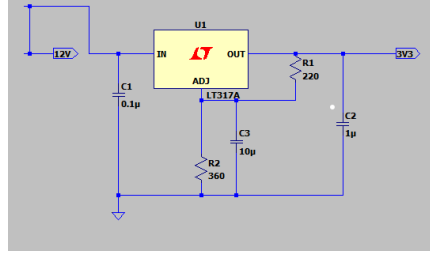


Figure 1.2: LM317 full 3.3V regulator circuit

Current requirements:

For a voltage drop of 8.7V and an output voltage of 3.3V the LM317 can supply up to 2.2A [1]- well above the needs of low power devices like the ESP board drawing a few mA at most [5]. The other components to be implemented will not sum to draw near this current.

Key regulator conditions:

To ensure specified and stable regulator operation the total load current must be above 3.5mA and below 2.2mA which is expected as per literature. The designed output voltage is 3.3V which is between the required range of 1.2V and 37V

Implementing capacitive filters to reduce noise:

Capacitors are implemented on the input and output nodes in order to improve transience and steady-state stability respectively. Another capacitor, C3, is also implemented parallel to R2, visible in figure 1.2, to further improve the stability of the system. By improving the stability the system noise caused by the power supply and environment is mitigated. These capacitors act as filters to remove noise at non-DC frequencies. Having precise values for these capacitors is not a primary concern as they are used for stability and hence standard application values are used. This, according to the LM317 datasheet [1], is $C_{in} = 0.1\mu F$ and $C_{out} = 1\mu F$. For the capacitor C3, an appropriately stable value is $10\mu F$.

Choosing Resistor Values

A choice must then be made for an R1 value, and by implication an R2 value, that is appropriate for the circuit. If this initial value is chosen to be too high, the steady-state response will be noisy but if too low, cause high power usage. A balanced value, as per the LM317 datasheet [1], is $R1 = 240\Omega$. The nearest standard resistor of 220Ω is chosen.

The following formula, derived from [1], allows control of the output voltage and applies to the final regulator circuit, shown in figure 1.2:

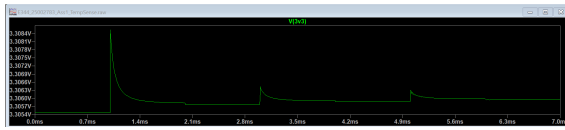
$$V_{out} = 1.25 \left(1 + \frac{R2}{R1} \right) + I_{adj} \cdot R2 \quad (1.1)$$

Calculating Resistor Values

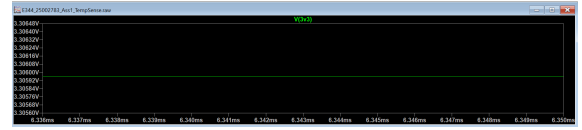
As per the LM317 datasheet [1], the current I_{adj} has a maximum value of $100\mu A$ and a typical value of $50\mu A$. Using the typical current and an output voltage of 3.3V as specified, R2 is found with the control equation to be 357.65Ω and this will be approximated with a series connection between a 330Ω and a 33Ω standard resistor.

1.3. Simulated results

During transience the voltage ranged between 3.305V to 3.309V as per figure 1.3a and tended to a steady state voltage of 3.306V as per figure ???. This is within the 0.5% tolerance. Note: the label net "3V3" refers to the voltage at the load.



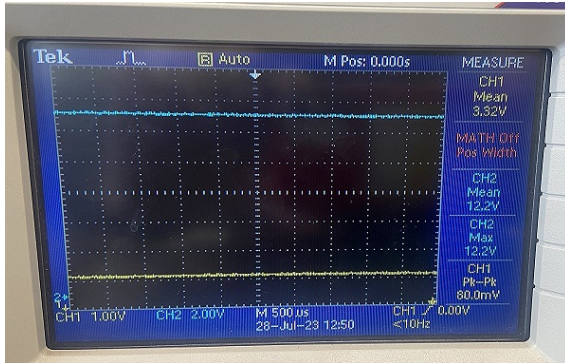
(a) Transient voltage response at load



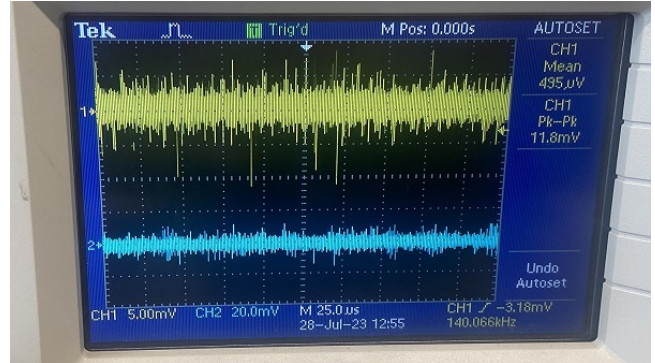
(b) Steady-state load voltage

1.4. Measured results

As specified by the module coordinator, there is a 2% design tolerance on the output voltage. This corresponds to an acceptable range between 3.234 to 3.366V which was met as seen in the figures below. This was tested with a 12V rated input wall adaptor. Channel 1 (yellow) is the output node for both pictures, the other is the input node.



(a) stable, acceptable 3.32V DC output on oscilloscope for a 12.2V input



(b) Output noise levels under AC coupling with a peak-peak voltage of 11.8mV

1.5. Summary

The 3.3V regulator system performed as expected in simulations within the 0.5% voltage tolerance and exhibited sufficiently low load currents. When built the system was within the new voltage tolerance of 2% as expected with a sufficiently low noise profile. In the context of the system there are no large drawbacks. If the system were to be made portable then the lower efficiency of the linear regulator would cause lower battery lifespans.

Chapter 2

Temperature sensor

2.1. Literature

An RTD is a temperature sensor that has an electrical resistance, which naturally increases with heat providing a positive and linear resistance-temperature relationship. This is in contrast to thermocouples which have similar applications but a non-linear relationship. The resistance of an RTD is encapsulated, in the case of the NB-PTCO-163, by the following linear approximation of the Callendar-Van Dusen equation as per [6], using the Temperature Resistance Coefficient of 3850ppm as per the as per RTD datasheet [7]:

$$R(T) = R_0(1 + \alpha(T - T_0)) \quad (2.1)$$

where $T_0 = 0^\circ\text{C}$, $\alpha = \frac{3850}{1000000}$, and $R_0 = 1000\ \Omega$ where R_0 is the resistance at temperature T_0 .

The choice of material used can affect the performance of the device. Platinum is most commonly used, as it is here, as it has a large input range of temperatures and a highly linear relationship. The construction also plays a role. Wire-wound RTDs have better stability but slower response times in comparison to the thin-film RTDs used in this project. An example of thin-film RTDs are included in figure 2.1 below for context. Vibration and moisture levels also have an effect on the devices performance [8].

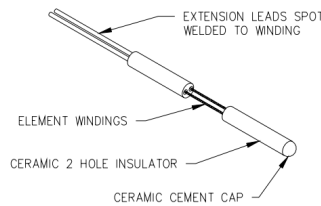


Figure 2.1: Thin Film RTD

When interfacing with an RTD its important to make sure there is limit self-heating. This can be done by ensuring low current flow through the device with appropriate Wheatstone choices and supply voltage [9]. Next the RTD resistance does not drastically change with respect to temperature as visible in the equation above. Thus, it is necessary to amplify this change to ensure accurate data capturing from the ADC. When amplifying this voltage - the voltage below the desired "start reading" temperature must be removed to ensure the amplification process does not attempt to cause excessive voltage levels. This can be done via a Wheatstone bridge where the resistors are equalized on both sides at 28°C . Finally, when doing all of this one must take care not to load any circuitry unknowingly. Here, loading refers to the unintended feedback of current from the final operational

amplifier into previous parts of the circuit i.e. the Wheatstone bridge which affects its operation.

Operational amplifiers are used to achieve the offsetting and scaling of the RTD circuitry. Types of operational amplifiers are discussed here as derived from [10].

1. Inverting amplifier: This configuration amplifies and inverts the signal. For e.g. you could use this to remove noise by first sampling the noise.
2. Non-inverting amplifier: This only amplifies the signal, for e.g. in volume control.
3. Differential amplifier: This amplifies the difference between two signals. This can be used to remove a DC offset before amplification as required in this project.
4. Summing amplifier: This amplifies the sum of two signals. For e.g. stereo to mono audio conversion with volume control.
5. Voltage follower (buffer): This is a special case of the non-inverting op amp where the gain is 1. This can be used to prevent feedback into a certain pathway i.e. loading.

2.2. Design

The designed circuit (to be explained) is as follows:

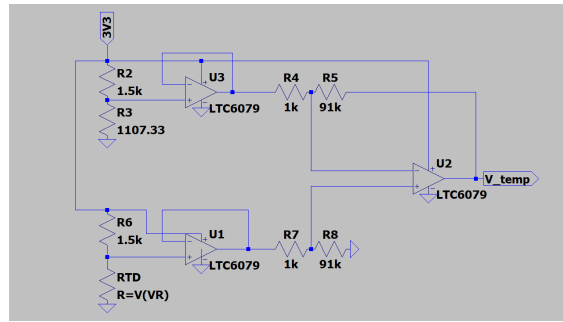


Figure 2.2: Analog temperature sensor configuration circuit

The ADC pins on the ESP board can take an absolute maximum of 3.6V as per the ESP datasheet [5]. The maximum specified operational amplifier voltage values as derived from the project is 3v and the minimum is 0V for the. This is within range and safe for the ADC pins. The value of the series resistor to the RTD should be high enough to limit current to the RTD which ensures limited self heating and regulator safety. However, the value must be low enough to cause enough of a current draw to not allow electromagnetic interference (noise) to become relatively substantial or cause the voltage changes to become so small that the amplifier becomes impractical to build. The other side of the Wheatstone simply matches the RTD and series resistor at a temperature of 28°C. Therefore, resistor values will be picked in excess of 500Ω and below 100kΩ to create a balance. Capacitors are not used to reduce noise as they will cause slower switching speeds and response times to changes in temperature.

Using equation 2.1 and the project specifications the following temperature implications are observed:

Table 2.1: Resistance and required output Voltage at Different Temperatures as per project specifications

Temperature (°C)	Resistance (Ohms)	Output Voltage (V)
28	1107.8	0
30	1115.5	0.5
35	1134.75	1.75
40	1154	3

In order to accomplish these, it is assumed that the circuit and sensor act linearly and any deviation to this will be in tolerance. A voltage Wheatstone circuit will match the voltage of the RTD sensor and its series resistor at 28°C so that there is 0V difference between the two sides at this temperature subtending no output voltage as per specifications. A 1500Ω series to RTD resistor is used, which is higher than the RTD's max resistance at the maximum project specified temperature, ensures the RTD output voltage is low enough to ensure no common mode voltage issues through the operational amplifier buffers. These buffers stop loading as described in literature. To reiterate they prevent current feedback from the final operational amplifier into the Wheatstone bridge. The RTD resistance at 28°C is 1107.8 Ω. To ensure accuracy, on the corresponding other side of the Wheatstone, the resistor is approximated with multiple standard resistors to achieve a Resistance of 1107.33Ω. The resistance range of the RTD from 28°C to 40°C must correspond to a voltage from 0V to 3V as per specifications. Before the amplification process, the Wheatstone ensures that this range is 0V to some mV (calculated later). This is then amplified to the specified range. Note that as per the circuitry, the maximum and minimum Wheatstone (Wheat) output voltages are achieved when the maximum and minimum temperatures (and consequentially RTD resistances) are present, as per project specifications. The gain is found as follows:

$$\text{gain} = \frac{V_{\text{desired_max}} - V_{\text{desired_min}}}{V_{\text{Wheatmax}} - V_{\text{Wheatmin}}} = \frac{3-0}{\left(\frac{1154}{1154+1500} \times 3.3\right) - \left(\frac{1115.5}{1115.5+1500} \times 3.3\right)} = 90.7923 \quad (2.2)$$

This is achieved by using a standard 1kΩ resistor and a 91kΩ resistor (which is made with a series combination of a 90kΩ and 1kΩ resistor) to achieve this gain.

2.3. Simulated Results

The simulation was linear and values as expected as per specifications.



Figure 2.3: Analog temperature sensor simulated output

The values are within specified tolerances (included in the table) for the given temperatures. They are stable for the given temperatures i.e. RTD resistance values. The exact values for each significant position on the graph are recorded in the table below:

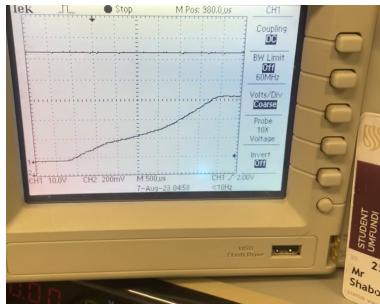
Table 2.2: Resistance and Output Voltage at Different Temperatures in simulation

Temperature ($^{\circ}\text{C}$)	Resistance (Ohms)	Output Voltage (V)	Tolerance Range (V)
0	1000	0	Not Applicable
30	1115.5	0.536	0.4 - 0.6
35	1134.75	1.792	1.45 - 2.05
40	1154	3.036	2.9-3.1
64.935	1250	3.272	3.25-3.3

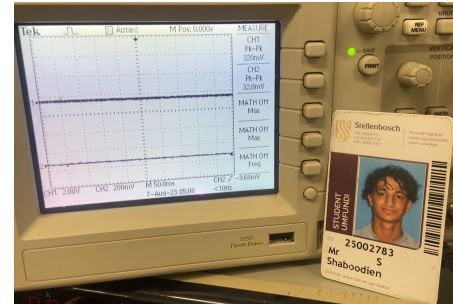
2.4. Measured Results

In figure 2.4a the voltage is 0V at room temperature then increases linearly from 0V at 28°C then starts linearly increasing until it stabilizes at around 3V at 40°C . These benchmark temperatures are achieved using two high power resistors set at a voltage corresponding to a specific steady-state temperatures. That voltage was found using the pre-calibrated digital temperature sensor. The flat line on the oscilloscope is to be ignored.

In figure 2.4b below, CH1 (top) represents the input voltage and CH2 the output voltage in AC coupling mode. As seen the output noise is significantly lower than the input noise implying the RTD circuit is robust to noise.



(a) Stable DC voltages over time, for two different temperatures



(b) Input (top) vs output noise

Figure 2.4: Sub-figures showing stable DC voltages and noise characteristics

2.5. Conclusion

As seen in this chapter the analog RTD sensor is implemented using a balanced Wheatstone bridge to offset the base temperature and then amplified to a usable voltage using decoupling amplifiers to prevent loading between the two.

Chapter 3

Temperature sensor

3.1. Literature

In this chapter the application of the load cell sensors in the system will be covered. The device will be calibrated in software. The load cell is a strain gauge. A strain gauge converts a mechanical force into a change in electrical resistance. This is a cause of the fact applied strain will cause a change in resistors path length. The cell consists of two resistors, one push and one pull. When compression via weight is applied, the push resistor's value increases whilst the pull decreases by the same value [11].

As per the load cell's datasheet [12], there is a 1mV/V gain for a 50kg applied load per cell. At no applied weight when the cell resistances are at a base resistance 1k Ω . In this situation, each resistor in either left or right half of the Wheatstone bridge has a voltage drop split equally between the 4 resistors causing a drop of $\frac{3.3}{4}V$ per resistor. Let the weight per cell equal w . $V_{noweighthalf}$ is the voltage drop across the bottom half of either side at no weight i.e $\frac{3.3}{2}V$. Using the data sheets formula from above, the absolute voltage change per weight at the specified voltage, in the configuration of figure 3.1a, for any single resistor in a cell is ΔV as follows:

$$\Delta V = 1mV * 3.3/4/50kg * w = 16.5\mu * w \text{ V} \quad (3.1)$$

This represents the given data sheet resistor's voltage change per 50kg at 1volt normalized to the correct applied voltage and any per cell weight. Then, the output voltage at the left middle node, relative to ground, is as follows:

$$V_{out} = V_{noweighthalf} + V_{totalchange} = 3.3/2 + 4 \cdot \Delta V = 3.3 * \frac{(1000 + \Delta R) * 2}{((1000 + \Delta R) * 2 + (1000 - \Delta R) * 2)} \quad (3.2)$$

The lhs represents the change as per the given ΔV equations whilst the right hand side represents the voltage division representation involving ΔR . $4\Delta V$ was chosen since the bottom two resistors both increase by ΔV and the top 2 resistors both decrease by ΔV on the lhs leading to a $4\Delta V$ increase in nodal voltage. Solving for ΔR in terms of w , it is found that:

$$\Delta R = 40 \cdot w \cdot m \Omega \quad \therefore R_{pushorpull} = 1000 \pm 40 \cdot w \cdot m \Omega \quad (3.3)$$

Note m represents milli and w , weight per cell. The plus is for the resistance-weight relationship for a push resistor and the minus, for a pull resistor.

As per specifications, the voltage shall be 2.75V at 100kg (25kg x 4 cells) and 0V at no weight.

Thus, the voltage-weight relationship, in terms of the total weight on all 4 cells is:

$$\text{Voltage} = \frac{27.5}{1000} \times \text{weight_total } V \quad (3.4)$$

The performance of the cell can be affected by a variety of conditions. Firstly, electrical resistance is directly affected by temperature and one should interface with it at around room temperature. Next, performance may be affected if the load cells have different leading wire lengths and materials, or don't lie flat [13]. The devices may also be ill-calibrated due to manufacturing and require calibration in software [14].

When interfacing one should consider the load cell resistance changes, and thereby voltage drops, are very small per applied weight. This implies a low voltage change across the Wheatstone and large Electromagnetic interference which hampers The microcontrollers accuracy when reading these changes [14]. Hence, when interfacing with this device an amplification circuit is required to increase the voltage change across these resistors and the signal-to-noise ratio. Further, decoupling of the Wheatstone bridge and the gain amplification stage is required to prevent loading the Wheatstone bridge. This may be solved by unity gain operational amplifiers.

The interfacing with the load cells will be done using a Wheatstone bridge as per the circuit in figure 3.1a. The full circuit including the buffers and gain operational amplifier is shown in figure 3.1b

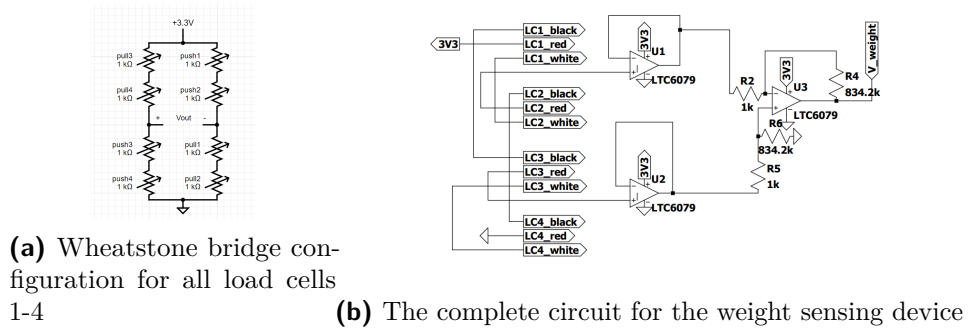


Figure 3.1: Combined figure

Firstly, before designing the circuit, a bit of context on how a Wheatstone bridge works and how to use it is required. In figure 3.1a, one can see the different push and pull resistors for all load cells in the Wheatstone bridge. They are configured to be balanced for the base values and provide precise voltage control. This means the Wheatstone works as follows: at no applied weight, all the resistors read $1000k\Omega$, and the centre (output) nodes read the same voltage i.e they are balanced on both sides implying an output of 0V.

As the weight is applied, the push resistors will increase and the pull resistors decrease as per formula 3.3. On the lhs, the voltage drop across the bottom two resistors increases by $2\Delta V$ and the top half's decrease by $2\Delta V$. This implies the middle lhs node increases from 1.65V to $1.65V + 4 \cdot \Delta V$. On the right hand side node the push and pull resistors are configured in reverse implying that instead, the voltage at the middle node will decrease by $4\Delta V$. Ultimately, as weight is applied $V_{outwheat}$, which measures the difference between the left and right centre nodes (as per the polarity in figure 3.1a) increases, from 0V when no weight is applied, to $8\Delta V$. At maximum designed weight of $w=25\text{kg}$ per cell, $V_{outwheatmax} = 8\Delta V = 8 \cdot 16.5\mu \cdot 25 = 3.3mV$ as per formula 3.1. This implies

the output range of the Wheatstone bridge is from 0V to 3.3mV. The configurations of the buffers to prevent loading and the differential operational amplifier are detailed in chapter 2.

3.2. Design

As specified, the output voltage will be from a minimum of 0V to a maximum of 2.75V. The op amps that are being used are rail to rail meaning they can output very close to the rail voltages. The 0V minimum can be supplied since the negative supply rail is 0V and the maximum op amp output of 2.75V can be supplied since the positive supply rail is 3.3V. Therefore, in relation to the acceptable range of the operational amplifier circuitry, the minimum and maximum op amp input voltage ranges are within the rail and common mode voltage allowances. Next, the minimum and maximum voltages of the ADC pins on the microcontroller are 0 and 3.3V respectively, as per the datasheet [5]. As noted above, the gain op amp output is 0-2.75V which is within the acceptable range of the ADC pins.

The output range of the device was covered in literature. However to restate, the output range of the Wheatstone bridge is from 0V to, as per the circuit configuration and literature, the sum of the absolute weight driven changes in voltages for all 8 resistors = $8\Delta V$. As a consequence of formula 3.1 and as explained in literature, the output voltage of the Wheatstone when each cell experiences a specified maximum weight of 25kg, is 3.3mV. Hence, the output range of the Wheatstone is 0-3.3mV.

Now, the gain required to amplify the circuit shown in figure 3.1b is as follows:

$$\text{Gain} = \frac{\text{desired_Output_range}}{\text{Wheatstone_Output_range}} = \frac{2.75 - 0}{3.3 \cdot 10^{-3} - 0} = 833.3333 \quad (3.5)$$

This gain is approximated using a standard 1k Ω resistor and an 833.2k Ω (a series connection between a standard 820k Ω , 12k Ω , 1.2k Ω) which is configured as per the circuit in figure 3.1b. The lower value, 1k Ω was chosen to be a balance. If it were too low the current draw and power consumption of the circuit would be unacceptable. However, if too high the power consumption would be so low that the effects of electromagnetic interference i.e. noise would become very prominent due to the low currents. The value was chosen such that the circuit will only consume one or two mA at maximum draw however that the draw is still enough to have a high signal-to-noise ratio to reduce the effects of noise.

3.3. Simulation

The simulation in LTspice showed that the voltages for the different applied weights resulted in the appropriate voltage. Note that for these simulations the approximated gain op amp resistor of 833.2k Ω is used.

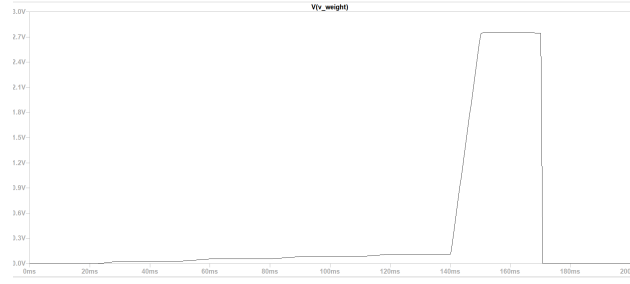
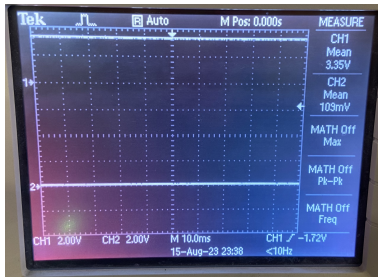


Figure 3.2: Simulated results for different weights over time

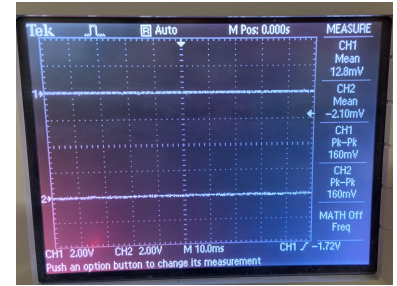
When measured, these voltage values were all within tolerance.

3.4. Measured Results

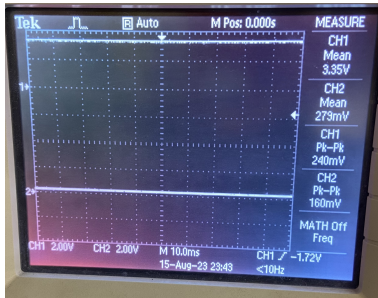
The following results are tested at 2 different weights. These are 4kg, 10kg. The output voltage of the weight system will be compared against the input power rail of the system on the oscilloscope in both DC and AC coupling. The top bar, channel 1, is the power rail input and the other is the output of the weight system for all pictures.



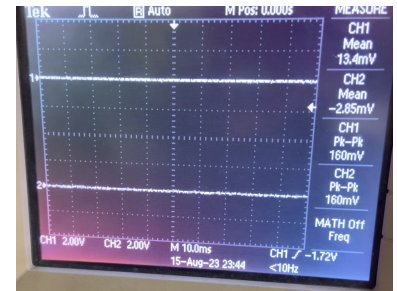
(a) DC voltage under 4kg load



(b) AC noise under 4kg load



(c) DC voltage under 10kg load



(d) AC noise under 10kg load

As per the weight-voltage formula, the expected DC voltage at 4kg;10kg is 110mV;275mV respectively. The voltage in the figures are 109mV and 279V respectively which is within tolerance. The AC coupling readings are in the low hundred mVs and the output noise is not above that of the input noise, implying stability.

3.5. Conclusion

As required, the weight system reads a weight from 0kg to 100kg and accurately outputs a voltage from 0V to 2.75V to the Arduino which is displayed on the OLED.

Chapter 4

Pedometer

4.1. Literature

An accelerometer is a device which translates acceleration into an electrical signal. When the device experiences acceleration, a mass suspended by a spring moves changing the resistance of the electromechanical system - leading to a change in voltage. This voltage is then outputted per axis at one of the three data lines as per the datasheet [15]. As per the accelerometer datasheet [15], the accelerometer has a sensitivity of 300mV/g at a supply voltage of 3V. Linearly extrapolating this - 330mV/g will be the sensitivity for a 3.3V supply. This sensitivity implies a positive or negative change of that voltage for every g (9.81m/s^2) applied will occur depending on the direction of acceleration. For a step there is a positive and negative acceleration and thus only the positive acceleration will be considered forward to ensure not double counting steps. The per-axis (without gravity) base voltage is 1.65V i.e half the supply voltage. In the z direction gravity applies 1g downwards constantly resulting in a base voltage of $1.65 + 0.33$ V. These base voltages are accounted for in software. The total voltage relationship as a function of acceleration can be summarized in the following vector formula:

$$\bar{V}(x, y, z) = (0.33 \cdot a_x + 1.65)\bar{a}_x + (0.33 \cdot a_y + 1.65)\bar{a}_y + (0.33 \cdot a_z + 1.65 + 0.33)\bar{a}_z \quad (4.1)$$

where: \bar{V} is the voltage vector for each axis, a is the magnitude of the applied acceleration in that direction, in g, and \bar{a} is the unit vector in the respective axis. Note that each directional magnitude corresponds to a voltage in one of the 3 data cables on the accelerometer.

The following aspects may affect the performance of the accelerometer: 1. If one chooses to remove an offset related to gravity from the z axis in specific it is necessary to then keep the device orientated perfectly in both static conditions and throughout the dynamic movement.

3. One should also consider noise on these channels. This can cause error and parallel capacitors can be used when interfacing to reduce this noise. This can be placed on the data lines for stability and the power supply pins to decouple it from power supply noise.

4. Response time may affect performance. Capacitors can be placed in parallel to each data line in order to control the Bandwidth-noise relationship. If the Bandwidth (and response time) is too high, the noise will be high but conversely, if it is too low the response time will be significantly slower. A balance is required to account for response time and noise. Hence, a $0.01\mu\text{F}$ capacitor per data line is chosen to have a low noise and still speedy response implied by a 500Hz Bandwidth as per the accelerometer datasheet [15].

Analysing the typical acceleration values for walking and running is a highly complicated and

multifaceted topic. This involves acceleration and deceleration points which are different per body part. However, in this case a simplified model is taken by only considering the total 3-dimensional magnitude of the mean peak positive acceleration (MPPA) of the hip (where a phone pedometer is commonly placed). This information is found in article [16] and subtends the following values:

Table 4.1: MPPA Values for Walking and Running

Activity	MPPA (m/s^2)	MPPA (g)
Walking	3.3	0.43
Running	5.2	0.64

4.2. Design

As noted in the literature the expected walking and running peak acceleration mean values are 0.43 and 0.64g respectively.

Further, as previously explained, the base voltages are half the supply voltage where gravity causes the z axis to further increase by 0.33V - the voltage sensitivity per g. The voltage vector equation 4.1 is shown again below, and note the values are explained in literature.

$$\bar{V}(x, y, z) = (0.33 \cdot a_x + 1.65)\bar{a}_x + (0.33 \cdot a_y + 1.65)\bar{a}_y + (0.33 \cdot a_z + 1.65 + 0.33)\bar{a}_z \quad (4.2)$$

As per project specifications, the accelerometer will be tested in a single direction at a time. Only the positive acceleration will be considered to ensure not double counting steps. Hence, the expected voltages will be calculated for no acceleration, a step-equivalent positive walking and running acceleration in an individual axis. This can be solved by subbing in 0, 0.43g, and 0.64g into the above formula for all axes. This results in the following expected voltage values per axis for no acceleration, a step and a run in that direction:

Table 4.2: Expected voltage values for different positive accelerations in each direction

Direction	No acceleration [V]	Step acceleration [V]	Running acceleration [V]
X	1.65	1.792	1.861
Y	1.65	1.792	1.861
Z	1.98	2.122	2.191

The voltage which counts as a step will naturally be considered as counting as a step. Hence, the acceptable threshold voltages will be chosen to be slightly lower than a step to ensure slightly slower steps are also read. As per the table, these individual axis rounded down voltages for x,y,z will be 1.6,1.6,1.9V respectively. As explained later, the code checks for the change in magnitude to account for non-perfect orientation cases and measurement errors. This results in an exact threshold voltage change for walking (0.43g) of $\Delta V = 0.4g \cdot 0.33V/g = 0.1419V$. This is rounded down to 130mV to account for slower steps.

To reduce noise, parallel capacitors are placed in parallel to the data lines to balance the response time and noise - more on this in literature. As such, $0.01\mu\text{F}$ capacitors are placed in parallel to each data line allowing a response time corresponding to a bandwidth of 500Hz. Further, to decouple the device from power supply noise a $0.1\mu\text{F}$ capacitor is placed in parallel to the power supply pin.

The current draw for the ADXL335 is between $350\mu\text{A}$ and $375\mu\text{A}$ for a supply voltage between 3V and 3.6V respectively. Hence, it can be said that the current draw is insignificant enough to not overload the regulators or the power supply.

No circuitry design was made nor subsequent simulations. The accelerometer, data pin and power supply parallel capacitors are trivial enough to not require this. On a higher level, the software design involved reading the ADC values, calculating the magnitude and seeing if there is a large enough difference which increments the step counter.

Below in figure 4.1 is a flow diagram of the software. Explanation will follow

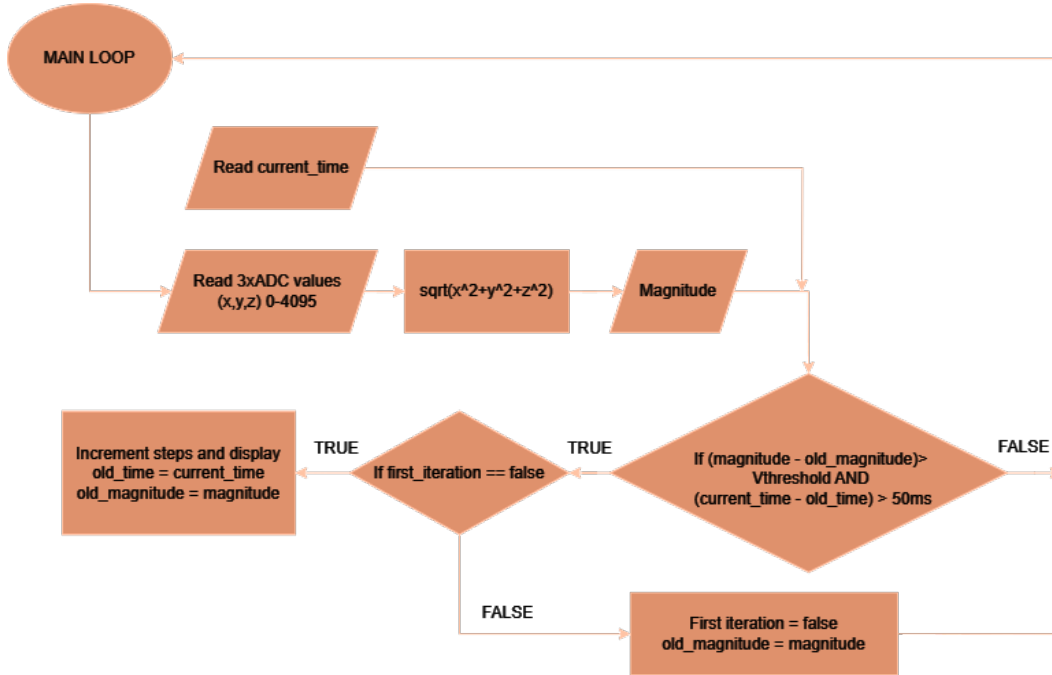


Figure 4.1: Flow diagram of the code

On a higher level, the code calculates the magnitude of the read ADC values. If the difference between loop values are greater than the threshold voltage as an ADC value ($\frac{0.133.3}{1620} \cdot 4095 = 1620 \text{ on ADC}$) and a safety time period has expired, then a step is read and the step count is updated. Instead of negating the base and gravitational constant voltage offsets, a different approach is used. This is because reducing by offsets can result in error if the offsets are measured even slightly incorrectly. The code will instead consider the difference between the current and previous loop's magnitude values ($\sqrt{x^2 + y^2 + z^2}$). This is because the offset is constant and hence the difference between the current and previous values are equivalent to the difference between the current and previous offsets. This is a more accurate way of judging the step count. Each step has positive and negative accelerations and only the positive should be read to ensure

no double readings. Further, noise and vibration can also cause false readings. Hence, to reduce false and extra readings - a non-blocking time delay is added before a subsequent reading may be registered as a step.

Finally, the first loop iteration will be ignored as the old magnitude variable will be 0 and the current magnitude of the voltage will not as per equation 4.1.

4.3. Measurements

Below, each axis' waveforms are measured for a step-like acceleration while holding the device upright in figure 4.2 a-c. Figure 4.2D shows the noise level in AC coupling mode (Channel 1 - top) of the output versus input (Channel 2) for the x-axis, all other data lines are similar.

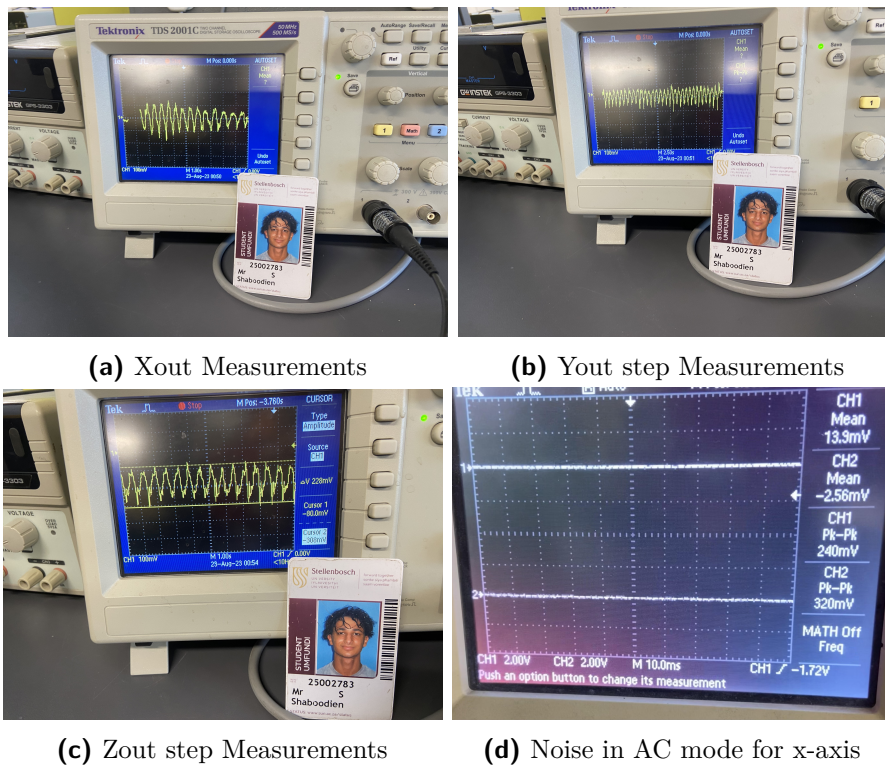


Figure 4.2: Step measurements for each axis and noise measurement

Below is a table showing how many steps were measured on the output at the OLED for a set amount of step movements:

Axis	Shakes per Axis	Steps per Axis
X	10	9
Y	10	10
Z	10	9

4.4. Conclusion

The accelerometer uses the Wheatstone bridge and signal conditioning to increment the steps via the Arduino.

Chapter 5

Heartbeat Sensor

5.1. Literature

Light based heart rate sensors are commonly used today. They work by essentially passing light through your skin and measuring the amount of a specific spectrum of light reflected back. There are mainly two types of heart rate measuring modes. The first is spectroscopy which beams an array of different wavelengths of light at the target area and measures the amount of each wavelength that returns. Different compounds in the body will absorb different wavelengths differently. As such, peaks and troughs at certain frequencies in the returned light can give us insight into the types and amounts of compounds present. oxyhemoglobin increases during a heartbeat, a compound which absorbs green light predominantly, these dips in the amount of green light reflected can be used to identify heartbeats [17]. The second mode is Photoplethysmography (PPG). This beams light at the target area, generally green light and IR are used for this. Although X-rays and other high frequency rays can penetrate deeper they are not used due to their risk of damaging cells [18]. As the heart pumps blood through the capillaries, there is an increase in blood volume. This absorbs some of the beamed light causing less reflected light. This change can be converted to an electrical signal using a phototransistor or photoresistor and used to read heartbeats.

The first type of sensor is a phototransistor which causes a voltage and current to be induced upon the base [19]. This base current naturally controls a larger collector current allowing for a larger change in voltage to be read across the collector or emitter. This is beneficial for accurate reading and does not require much circuitry.

The second is a Light dependent resistor. As the incoming light increases its resistance drops. To implement this a voltage divider circuit is commonly used. This component is cheaper but less accurate.

Due to the accuracy a phototransistor, the QSD123 [19], is used for this project. Additionally, the IR light source, the QED123 [20], will be used due to its penetrating ability over that of white light.

The following diagram shows the working of PPG. The blood volume increases during the heartbeat - resulting in less light reflected back.

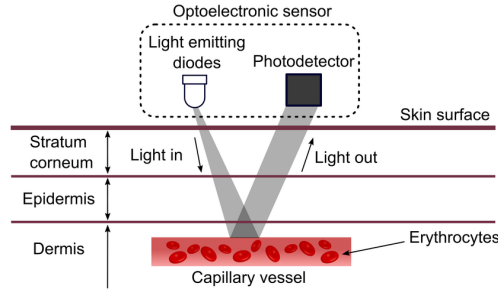


Figure 5.1: Working of PPG heart rate sensor

5.2. Design

5.2.1. Heart rate sensor circuit

The phototransistor will be in series with a $1.2\text{k}\Omega$ resistor and tuned with a potentiometer to cause a central node voltage of 1.65V . This ensures current limiting and the voltages oscillates at the middle of the power supply range. That means the operational amplifiers will not inadvertently cutoff any AC troughs. The IR light source is in series with a $50\ \Omega$ to limit the current to $3.3/60 = 55\text{mA}$. This is below the absolute maximum of the IR light which is 60mA [20]. The circuit is visible below in figure 5.2

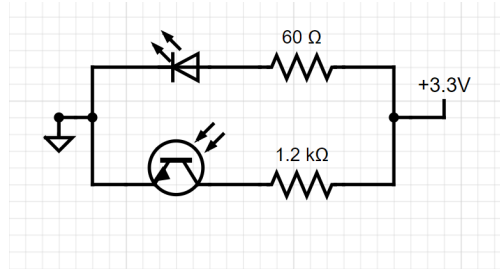


Figure 5.2: Heart Rate Sensor Circuit

The sensor output signal (between the phototransistor and the $1.2\text{k}\Omega$ resistor) will be conditioned through the following three stages (note that the associated circuit diagram appears thereafter):

5.2.2. Filter stage

This will use an active low-pass and active high-pass filter to only allow a passband through. This passband will correspond to a natural human Beats per Minute (BPM) range. This range will be 40-200BPM or equivalently, 0.5 to 4Hz. This will remove all noise outside of this spectrum and any DC components. This is necessary as the reflected light is distorted and noisy and there is a low signal to noise ratio. The DC and noise elements should not be amplified and so they are filtered out first. The unity gain operational amplifiers, used in the filters, also act as buffers, preventing reverse emf into the sensor i.e. loading.

For both active filters, the following equation applies.

$$f_{\text{cutoff}} = \frac{1}{2\pi RC}$$

Both filters will use a $1\mu\text{F}$ resistor. The low pass filter must let all signals below 4 Hz (its cutoff frequency) through implying a resistance of $39.8\text{ k}\Omega$ as per the equation. Similarly, the high pass allows all signals above 0.5Hz through implying a resistance of $318.3\text{ k}\Omega$. These are approximated using the closest standard resistors as slight variations to the cutoff frequency will not affect the operation due to the already large BPM range.

5.2.3. Gain stage

The filters remove most of the noise however a low signal size will still be susceptible to oscillations (causing extra comparator pulses) due to the relative size of EMI. This is solved by increasing the signal size from its current range to a large enough range. Since finger movements cause deviation, the output of the sensor has a range from 0 to between 3 and 6mV. As such the 6mV will be scaled to 3V and the 3mV will naturally become 1.5V. The trigger in the next stages will account for this. This desired range will be 3V peak-to-peak and the current range is 0-6mV peak-to-peak. The gain is hence $3\text{V}/6\text{mV} = 500$.

5.2.4. Comparator stage

Since the new range of the output signal of the heartbeat sensor is from 0 to between 1.5 and 3V, the comparator shall aim to read a trigger (will trigger low above this trigger as per requirements) below these voltages. The amount below this will determine the pulse width which is largely irrelevant due to only reading the time between pulses to calculate BPM. As such the high/low voltage trigger level will be set at 1.2V, ensuring all peaks are read and a relatively even pulse width. The signal is also required to be inverted, this is done by connecting the output of the gain operational amplifier to the negative terminal. A reference voltage of 1.2V is then applied to the positive terminal. For e.g. when the gain amp output is higher than the reference voltage (during a spike) a negative differential will be induced on the terminals and vice versa. Since there is no feedback, the operation amplifier will have infinite gain resulting in either a negative rail output voltage of 0V (low) or conversely 3.3V (high). These pulses will be inputted to the arduino where a moving average of the time between the rising edges of consecutive pulses will be converted to a BPM value and outputted.

The full conditioning circuit is thus as follows in figure 5.3

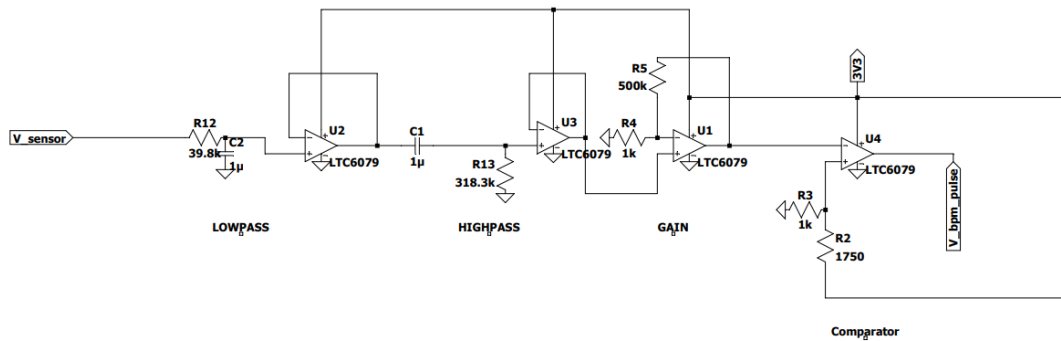


Figure 5.3: Heart Rate signal Conditioning Circuit

5.3. Simulated Results

For simulation, the authors heartbeat is recorded on the oscilloscope as seen below in figure 5.4, using the built sensor circuit, and imported as the input of the simulation. The simulation yields the following output, seen in figure 5.5, where the pulses correspond inversely and correctly to the peaks of the authors heart rate signal. This verifies that the sensor circuit works as expected to a realistic heart rate signal with noise and amplitude variances due to finger movements.

Authors heart rate signal:

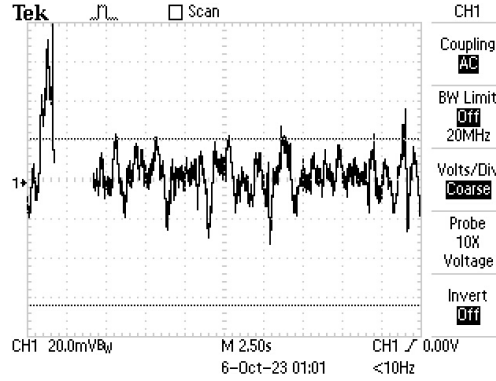


Figure 5.4: Heart Rate input signal of author

Output of simulation plotted against filtered and amplified heartbeat signal:

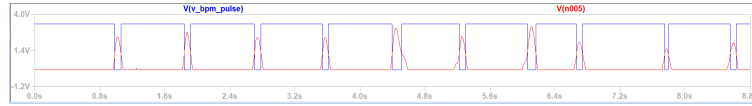


Figure 5.5: Simulation output vs conditioned input

The simulation total (input) current has a peak to peak current under 0.5mA which is below the specified maximum current. The current waveform is as follows:

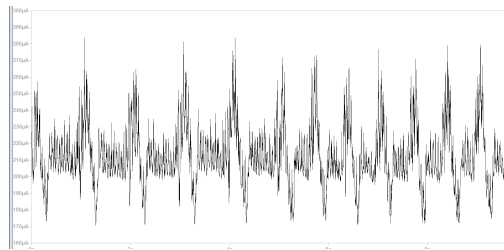


Figure 5.6: Simulation circuitry current usage

5.4. Measured Results

The reading in figure 5.7 shows the output pulses when a finger is in contact with the sensor, in comparison to the signal variation at the output of the sensor circuit. The pulses correctly inversely correspond to the input signal waveforms.

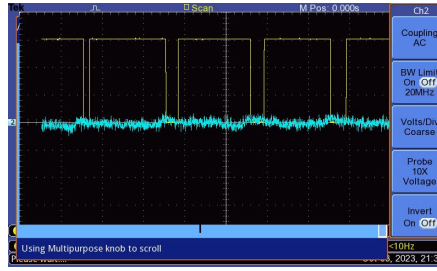


Figure 5.7: Measured pulse output vs heart rate input

Figure 5.8 shows the input vs output noise, using AC coupling, on the input power rail versus that of the output pulses. The output noise is correctly significantly less than that of the input

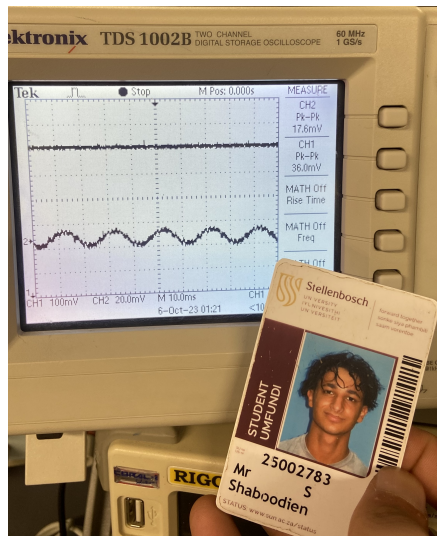


Figure 5.8: Input (CH1) vs output (CH2) noise

5.5. Conclusion

This chapter shows how light can be useful too to measure heart rate and illustrates the potential to create a portable, low power, space-efficient device. Its important to consider ways to mitigate noise and ensure limited sensor to target area movement or robustness to any movement to ensure accuracy.

Chapter 6

System Overview

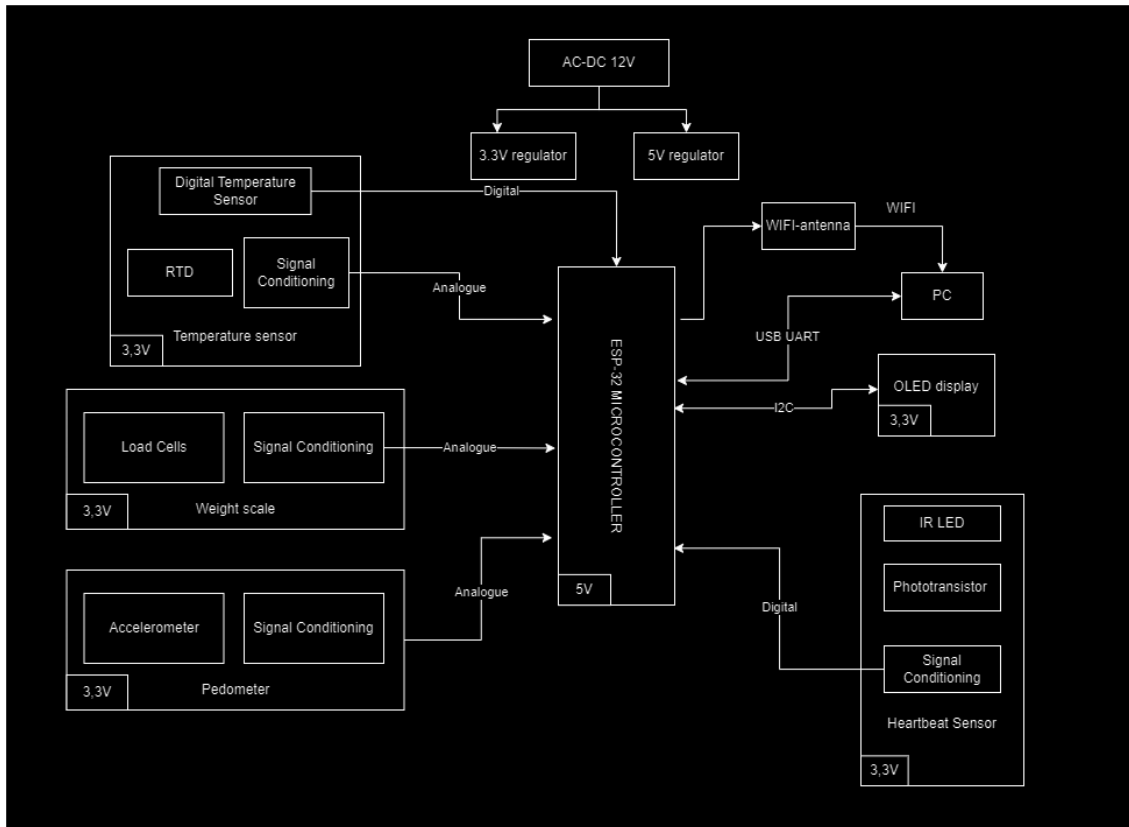


Figure 6.1: System Overview

The E-Design 344 project involves the design and implementation of a low-powered multi-aspect analogue health monitoring system. There are two regulators which convert 12V to 5V and 3.3V. The ESP-32 Arduino Framework microcontroller is the central unit which uses basic software to input and output signals to a user-friendly PC GUI via WiFi or via I2C on the OLED display. The system contains a temperature sensor, weight scale, digital pedometer, and heartbeat sensor. These involve circuitry to realize the sensor changes and conditioning to clarify the signals for the Arduino.

Bibliography

- [1] *1.2 V to 37 V adjustable voltage regulators*, ST life.augmented, 12 2021, rev. 22.
- [2] *LM2576 Series*, TIGER ELECTRONIC CO.,LTD, 01 2013, rev. 1.
- [3] H. Zhang, “AN-140: Basic Concepts of Linear Regulator and Switching Mode Power Supplies,” 2018.
- [4] “Bobshop formerly bid or buy,” Website.
- [5] *ESP32-C3 series*, Espressif Systems (Shanghai) Co., 10 2021, version. 1.1.
- [6] M. Looney, “RTD Interfacing and Linearization,” 2011.
- [7] *Platinum Thin Film RTD Temperature Element*, TE connectivity, 05 2015.
- [8] P. S. Limited, “What Is RTD Sensor And How Does It Work?” 2020.
- [9] Variohm, “How does an RTD work?” 2019.
- [10] N. Dubey, “Types of Op Amp,” 10 2022.
- [11] FUTEK, “What is a strain gauge load cell,” 07 2018.
- [12] *SEN 10245 load cell*, Sparkfun, 08 2016.
- [13] I. F. Measurements, “How Do Load Cells Work?” 01 2023.
- [14] K. Vining, “The Five Critical Factors of Load Cell Quality,” 09 2020.
- [15] *Small, Low Power, 3-Axis ± 3 g Accelerometer*, AnalogDevices, 05 2015, rEV. B.
- [16] M. A. Lafortune, “Three-dimensional acceleration during walking and running,” 03 2004.
- [17] F. Jabr, “How Does a Spectrograph Work?” 12 2012.
- [18] I. J. B. Bioelectron, “A review on wearable photoplethysmography sensors ,” 04 2018.
- [19] Onsemi, “Plastic Silicon Infrared Phototransistor,” 05 2010.
- [20] —, “Plastic Infrared Light Emitting Diode,” 08 2008.

Appendix A

Social contract



UNIVERSITEIT•STELLENBOSCH•UNIVERSITY
jou kennisvennoot • your knowledge partner

E-design 344 Social Contract

2023

The purpose of this document is to establish commitment between the student and the organisers of E344. Beyond the commitment made here, it is not binding.

In the months preceeding the term, the lecturer (Thinus Booysen) and a few paid helpers (Jacques Wüst, and Michael Ritchie) spent countless hours to prepare for E344 to ensure that you get your money's worth, that you are enabled to learn from the module, and demonstrate and be assessed on your skills. We commit to prepare the assignments, to set the assessments fairly, to be reasonably available, and to provide feedback and support as best and fast we can. We will work hard to give you the best opportunity to learn from and pass analogue electronic design E344.

I, Sameer Shaboodien have registered for E344 of my own volition with the intention to learn of and be assessed on the principals of analogue electronic design. Despite the potential publication online of supplementary videos on specific topics, I acknowledge that I am expected to attend the scheduled lectures to make the most of these appointments and learning opportunities. Moreover, I realise I am expected to spend the additional requisite number of hours on E344 as specified in the yearbook.

I acknowledge that E344 is an important part of my journey to becoming a professional engineer, and that my conduct should be reflective thereof. This includes doing and submitting my own work, working hard, starting on time, and assimilating as much information as possible. It also includes showing respect towards the University's equipment, staff, and their time.

Prof. MJ (Thinus) Booysen

Student number: 2500783

Signature: MJ Booysen
Digitally signed by MJ Booysen
Date: 2023.07.22
16:42:25 +02'00'

Signature:

Date: 22 Jul 2023 Date: 27 July 2023

Appendix B

GitHub Activity Heatmap



Appendix C

Reference figures